

# PICO: Pipeline Inference Framework for Versatile CNNs on Diverse Mobile Devices

Xiang Yang, Zikang Xu, Qi Qi, Jingyu Wang, Haifeng Sun, Jianxin Liao, and Song Guo, *Fellow, IEEE*

**Abstract**—Recent researches in artificial intelligence have proposed versatile convolutional neural networks (CNN) with different structures and substantially improved the accuracy of various intelligent applications. Nevertheless, the CNN inference imposes heavy computation overhead on mobile devices, but uploading the large volume of raw data to the cloud causes significant network latency. Motivated by the spatial independence of convolution operation, we propose pipeline cooperation (PICO) framework to accelerate CNN inference using multiple diverse mobile devices in this paper. PICO divides the CNN and mobile devices into several stages and combines them into an inference pipeline. PICO faces three main challenges: (1) Parallelizing the convolution operation introduces redundant calculation. (2) The partition is greatly complicated since the structures of many CNNs are directed acyclic graphs (DAG). (3) The mobile devices own diverse computing resources. In response to these issues, a two-step optimization is proposed based on deep analysis. We first orchestrate the DAG into sequential pieces, then divides these pieces and devices into stages. The optimization goal is to minimize the redundant calculation during partition and maximize the throughput. In our experiment with 2 ~ 8 RaspberryPi devices, the throughput can be improved by 1.8 ~ 6.8× under different CPU frequencies.

**Index Terms**—Mobile Computing, Pipeline Inference, Model Deployment.

arXiv:2206.08662v1 [cs.DC] 17 Jun 2022

## 1 INTRODUCTION

RECENT years witness an explosive growth of mobile devices. The huge number of mobile devices provides a large volume of data (images, videos, etc.). Meanwhile, versatile convolution neural networks (CNN) with pre-trained parameters become powerful tools to make intelligent decisions using these raw data (*CNN inference*). Embedding CNN with mobile devices enables many intelligent applications to become reality, such as smart home, intelligent factory, and even automatic driving [1], [2].

One obstacle for the embedding is the resource-limited mobile devices. Compared with datacenter, the computing capability of mobile devices is not enough to perform CNN inference along. But on the contrary, the current wireless network is not prepared for transmitting the massive volume of raw data collected by these mobile devices. For example, an autopilot camera could capture more than 700 MB video record every second [3], and uploading all the video data to the datacenter will bring significant network latency. Moreover, uploading data from user devices to the cloud always brings concern about privacy [3].

Benefitted from the spatial independence of convolution operation, the input and output (*feature*) of convolutional (*conv*) layers can be split into several small tiles and executed on different devices. As a consequence, cooperative CNN inference on multiple mobile devices gains the attention of researchers recently [4], [5], [6]. During inference procedure, the data source (camera, sensors, etc.) captures raw data and splits it into tiles. These tiles are distributed to multiple

nearby mobile devices through a wireless network and executed independently using one or several layers. Then the data source is responsible to gather all the output tiles and stitch them to obtain the result. The procedure will be iterated multiple times until all layers are executed. Cooperative inference also protects user privacy since all the data stay in local. Moreover, the closer to the data source, the lower network latency it suffers. Compared with other strategies such as model compression and parameter pruning [7], [8], [9], cooperative inference neither loses the inference accuracy nor requires re-train the model.

However, despite all these benefits, there still leave some challenges that are not completely solved in previous works. Although the input feature can be parallel executed, (1) **the parallelism introduces redundant calculation** due to the property of CNN. The scalar in the output feature of one conv layer is calculated through a dot product with the conv kernel and a subregion of input feature. For most cases, the kernel size is bigger than  $1 \times 1$ , so that the input tiles of partitioned input feature will overlap with each other to guarantee the scalars at the edge of output tiles are correct. Moreover, the overlapped part will increase recursively when devices execute multiple layers during one iteration in the inference procedure, but the communication is expensive for mobile devices. As a consequence, the executed layers need to be carefully chosen. However, (2) **the structures of many CNNs are directed acyclic graphs (DAG)** rather than chains. ResNet34 [10] uses skip-connection technology that allows a layer to directly connects to another deeper layer. The structure of InceptionV3 [11] contains multiple branches to capture more information from the input feature. These complex structures lead to a huge number of possible choices. Previous works mainly focused on the chain structure [4], [5], [6], which is much easier than DAG. Compared with datacenter, (3) **the computing resources of**

- Xiang Yang, Zikang Xu, Qi Qi, Jingyu Wang, Haifeng Sun and Jianxin Liao are with the Institute of Network Technology, Beijing University of Posts and Telecommunications. E-mail: {yangxiang, xuzikang, qiqi8266, wangjingyu, hfsun}@bupt.edu.cn, jxlbupt@gmail.com.
- Song Guo is an IEEE Fellow (Computer Society) and an ACM Distinguished Member with the Department of Computing at The Hong Kong Polytechnic University. E-mail: cssongguo@comp.polyu.edu.hk

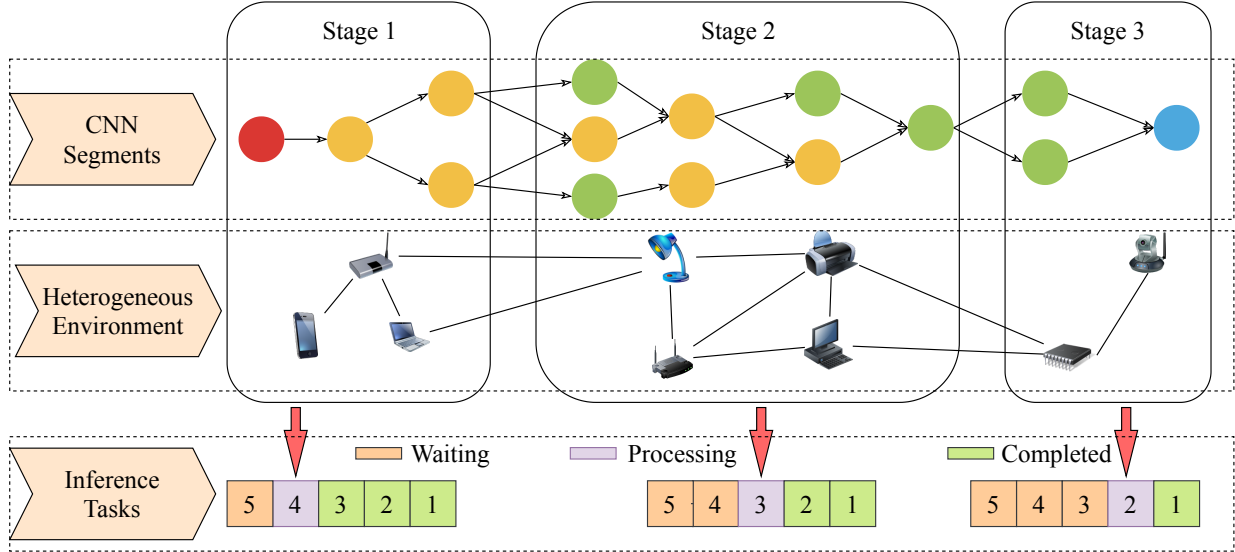


Fig. 1: A diagrammatic sketch of pipeline inference.

**mobile devices are diverse**, the heterogeneous environment also hinders the optimization for cooperative inference.

In this paper, we explore previous works about parallelizing the CNN inference and propose a pipeline cooperation (PICO) framework for accelerating the inference on diverse mobile devices. Fig. 1 plots a diagrammatic sketch of our framework. PICO divides the entire CNN graph and mobile devices into 3 *stages*. These stages compose an efficient inference pipeline. Since each stage owns a small segment of original CNN and a subset of mobile devices, both communication overhead and the redundant calculation can be significantly reduced. There are two important metrics for pipeline: *latency* and *period*. The first term is the sum of inference latencies of all stages and the last term is the longest latency among stages. Obviously decreasing the period tends to increase the latency. Our optimization goal is to minimize the redundant calculation and period (maximize throughput) meanwhile to keep the latency of the pipeline under a certain value.

We first formulate the pipeline inference, then we analyze the complexity of the optimization problem and find that it is NP-Hard to directly obtain the optimal result. Based on our analysis, PICO uses a two-step optimization to maximize the throughput. On the first step, we orchestrate the CNN graph into a sequence of *pieces*. These pieces have the minimum redundant calculation inside and compose the original CNN graph in a chain structure. Then we choose the best partition for these pieces and devices to construct the inference pipeline. The algorithms used in the above procedures are based on dynamic programming.

In our experiment we use 2 ~ 8 RaspberryPi to evaluate PICO framework. The throughput can be improved by 1.8 ~ 6.8 $\times$  under different CPU frequencies and number of devices.

In a nutshell, we make the following contributions:

- We present a pipeline cooperation (PICO) framework to accelerate CNN inference with diverse mobile devices.

- We propose an algorithm to split the complex CNN graph structure into more fine-grained pieces.
- We propose an algorithm to decide the optimal stage settings for inference pipeline which maximize the throughput.
- We apply our technique on a cluster consisting of Raspberry-Pi-based hardware and evaluate image recognition and object detection CNN models.

The rest of this paper is organized as follows: Section 2 provides background information of CNN and different parallelization strategies in mobile devices. Section 3 formulates the inference process and gives a cost model for further optimization. Section 4 and 5 describe our approach for finding near-optimal parallelization. Section 6 presents the results of our evaluation. Section 7 details the related work and Section 8 concludes.

## 2 BACKGROUND AND MOTIVATION

In this section, we briefly introduce the CNN inference and the current parallel schemes. Then we propose our pipeline cooperation scheme.

### 2.1 Procedure of CNN Inference

The convolution layer (*conv*) is the key module during CNN inference, Each conv layer own a set of kernels. To produces the output feature, conv layers uses their kernels to slide over the input feature received from the previous layer. Every movement of the kernel will produce a scalar in the output feature by a dot product between the weights of kernels and a small subregion of the input. The pooling layer (*pool*) performs a down-sampling operation. It is used to progressively reduce number of parameters, memory footprint and amount of computation in the network.

Conv operation is the biggest bottleneck. The Fig. 2 plots the computation and communication percentage by layer for two classic CNNs (VGG16 [12], YOLOv2 [13]). From the figure we can find conv layers dominate the consumption of



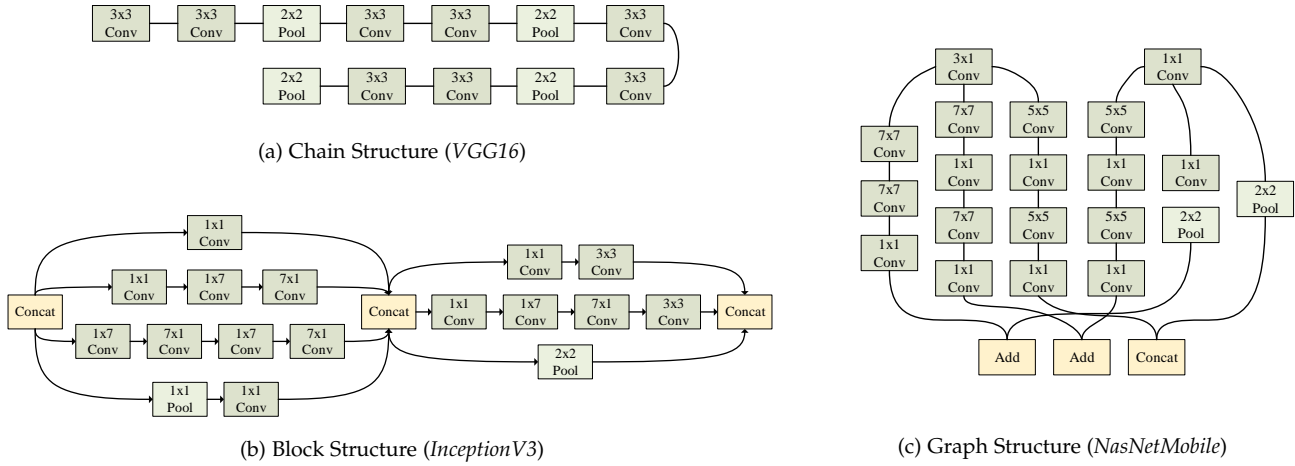


Fig. 3: CNNs with different structures: The chain structure is the simplest one which just put the neural layers into a sequence. Block structure replaces the element in chain structure from neural layer to block, each block can be seen as a directed acyclic graph (DAG). Graph structure can not be partitioned into blocks, the entire structure is a huge DAG.

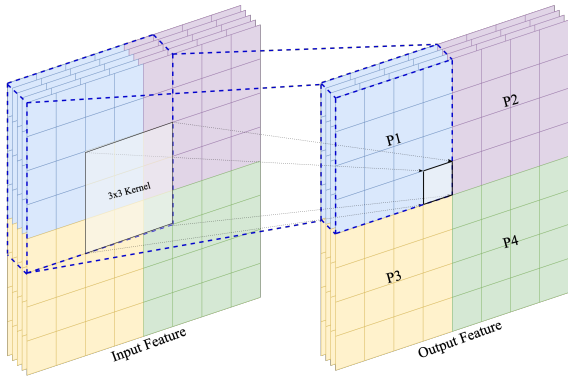


Fig. 4: Feature map partition strategy introduces redundant calculation.

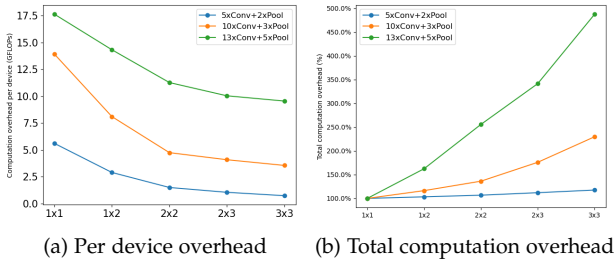


Fig. 5: Computation overhead with different partition settings.

the frequent communication among mobile devices causes inefficient performance. The redundant calculation also limits the cooperation of mobile devices for CNN inference. For fused-layer scheme, the redundant calculation quickly grows as the number of fused layers or devices increases. To give a detailed explanation, we evaluate the required floating-point operations (FLOPs) for VGG16 with different number of fused layers and mobile devices. Fig. 5a presents the FLOPs per device meanwhile Fig. 5b shows the sum of

FLOPs of all devices. We can find that fused-layer strategy performs well at start, but when the numbers of fused layers or devices increase, the redundant calculation quickly grows.

#### 2.4.2 Pipeline Inference

From the above discussion, the acceleration of CNN inference faces challenges when the number of devices or fused layers grows. For layer-wise scheme, the devices are idle in most time due to the frequent communication and expensive network latency. On the contrary, devices can keep running with the fused-layer scheme, but it is whistling to the wind since most calculation is redundant. Here we introduce *pipeline* scheme for parallelizing the CNN inference. This scheme divides both layers and mobile devices into several groups, as shown in Fig. 1. We refer such a group as *stage* in our description. The inference inside the stage uses fused-layer scheme and the entire CNN inference is performed stage by stage. If we set the number of stages to 1, The fused-layer scheme is a special case of the pipeline scheme. To maximize the inference throughput, the inference latency of every stage should be optimized as close as possible.

Using pipeline for inference has several advantages. (1) First, the communication overhead can be reduced since the calculated features only need to be synchronized among a subset of devices. (2) Second, the proportion of redundant calculation also decreases due to smaller numbers of layers and devices. (3) Third, each device owns a segment of CNN instead of entire model, which reduces the memory footprint.

The concept of pipeline is widely adopted in task scheduling [15], [16] which map multiple processors to an application composed by several tasks. However, pipeline meets difficulties when applied to CNN inference. The structure of CNN is a directed acyclic graph (DAG) rather than a chain, the mapping has to consider the data flow of DAG. Generally the number of layers in CNN is more than the number of devices, thus the mapping is many-to-many, and different mapping strategy also changes redundant

calculation. Moreover, the heterogeneous environment is also a big challenge.

### 3 SYSTEM MODEL

In this section, we define our optimization problem for pipeline inference.

#### 3.1 Problem Define

Generally speaking, our goal is to divide both CNN model with graph structure and mobile devices with heterogeneous computing resources into several stages properly, so that these stages could compose an inference pipeline that maximize the throughput.

##### 3.1.1 CNN With Graph Structure

We use an acyclic directed graph (DAG)  $\mathbb{G} : \langle \mathbb{V}, \mathbb{E} \rangle$  to represent a given CNN model. The vertex set  $\mathbb{V}$  contains all the neural layers and connector (e.g., Add and Contact in Fig. 3)  $l_i \in \mathbb{V}$ , and the elements  $(l_i, l_j)$  in the edge set  $\mathbb{E}$  denotes the data flow of CNN model  $\mathbb{G}$ . In particular,  $(l_i, l_j) \in \mathbb{E}$  means the output of layer  $l_i$  is the input of layer  $l_j$ . Since the CNN model will be executed as an inference pipeline with multiple stages, the  $\mathbb{G}$  also need to be split into multiple parts. We refer these parts as *segments*. A segment  $\mathcal{M} : \langle \mathcal{V}, \mathcal{E} \rangle$  is a subset of original DAG  $\mathbb{G}$ , where  $\mathcal{V} \subseteq \mathbb{V}$  and  $\mathcal{E} \subseteq \mathbb{E}$ .

Note the segment is *not* a regular smaller graph, since the edge set  $\mathcal{E}$  contains some vertices that are not included by  $\mathcal{V}$ . Take the Fig. 1 as an example, these segments on the top also contains edges that are connected with previous or next segments. Here we give some definitions of segment to simply our following modeling:

**Definition 1.** A subset  $\mathcal{M} : \langle \mathcal{V}, \mathcal{E} \rangle$  is a *segment* of original graph  $\mathbb{G} : \langle \mathbb{V}, \mathbb{E} \rangle$  if for all  $e : (u, v) \in \mathbb{E}$ , once  $u$  or  $v$  belongs to  $\mathcal{V}$ ,  $e$  also belongs to  $\mathcal{E}$ .

**Definition 2.** For a segment  $\mathcal{M} : \langle \mathcal{V}, \mathcal{E} \rangle$  and an edge  $(u, v) \in \mathcal{E}$ , if  $u \notin \mathcal{V}$ , then  $v$  is a *source* vertex of  $\mathcal{M}$ .

**Definition 3.** For a segment  $\mathcal{M} : \langle \mathcal{V}, \mathcal{E} \rangle$  and an edge  $(u, v) \in \mathcal{E}$ , if  $v \notin \mathcal{V}$ , then  $u$  is a *sink* vertex of  $\mathcal{M}$ .

##### 3.1.2 Optimization Goal

Given a heterogeneous cluster  $\mathbb{D}$ , where  $d_k \in \mathbb{D}$  is a computing device in the cluster. We assume the computing capacity  $\vartheta(d_k)$  of device  $d_k$  are known. In our practice, the  $\vartheta(d_k)$  denotes floating point operations per second (FLOPS). We also assume the bandwidth between all mobile devices is the same and is known as  $b$ . This assumption covers most cases when these devices under the same WLAN environment such as home and factory [6], [15].

For pipeline scheme,  $\mathcal{D} \subseteq \mathbb{D}$  is a subset of heterogeneous devices. Each device  $d_k \in \mathcal{D}$  owns a copy of model segment  $\mathcal{M}$  but is assigned to produce different region  $\mathcal{F}^k$  of the output feature map of all the sink vertex in  $\mathcal{M}$ . We use  $\mathcal{F}$  to present the set of all  $\mathcal{F}^k$  in  $\mathcal{D}$ . A stage  $\mathcal{S}$  can be represented as a tuple  $(\mathcal{M}, \mathcal{D}, \mathcal{F})$ . Let  $\mathbb{S}$  denote the set of stages composed by all the stages  $\mathcal{S}$  we defined above, the optimization objective is to find such a  $\mathcal{S}^*$  that satisfies:

$$\mathcal{S}^* = \arg \min_{\mathcal{T}(\mathbb{G}, \mathbb{D}, \mathbb{S}) \leq T_{lim}} \mathcal{P}(\mathbb{G}, \mathbb{D}, \mathbb{S}) \quad (1)$$

where  $\mathcal{T}(\mathbb{G}, \mathbb{D}, \mathbb{S})$  denotes the pipeline latency under specific stage configuration  $\mathbb{S}$  and  $\mathcal{P}(\mathbb{G}, \mathbb{D}, \mathbb{S})$  is the period of pipeline.  $T_{lim}$  is a hyperparameter that indicate the maximum inference latency we can accept.

#### 3.2 Cost Model

Here we represent our cost model to guide the optimization. First, we quantify the essential input feature size for every device in a stage. Then, we formulate the inference latency of every stage. Finally, we get the inference period and latency of entire pipeline using previous results.

##### 3.2.1 The Input Feature Size For Devices

Every device  $d_k$  owns a segment  $\mathcal{M} = \langle \mathcal{V}, \mathcal{E} \rangle$  and needs to produce correct output features  $\mathcal{F}^k$ . Once the  $\mathcal{M}$  and  $\mathcal{F}^k$  is given, we need to calculate the necessary input feature size for every layer  $l_i \in \mathcal{M}$ . The calculation had been discussed in [5], but it only considered models with chain structure. We will extend it into more complex graph structure here with a top-down algorithm.

To calculate the input feature size of layer  $l_i$ , we need to find all the edges  $(l_i, l_j)$  start from  $l_i$ . We can assume the input feature sizes of all  $l_j$  is already calculated. Since the input of  $l_j$  is just the output of  $l_i$ , the necessary output feature size of  $l_i$  can be denoted as:

$$w_i = \max \{w_{i \rightarrow j}\}, \quad h_i = \max \{h_{i \rightarrow j}\}. \quad (2)$$

Here we use  $w_i$  and  $h_i$  to denote the necessary width and height of the output feature size of  $l_i$ , meanwhile  $w_{i \rightarrow j}$  and  $h_{i \rightarrow j}$  is the input size of layer  $l_j$ .

Assume layer  $l_i$  has  $k_i^w \times k_i^h$  kernel size and  $s_i$  stride size, once the output feature size is determined, the height  $h_i$  and width  $w_i$  of input feature can be calculated using the following equation:

$$w_{* \rightarrow i} = (w_i - 1)s_i + k_i^w, \quad h_{* \rightarrow i} = (h_i - 1)s_i + k_i^h \quad (3)$$

where  $w_{* \rightarrow i}$  and  $h_{* \rightarrow i}$  is the input feature size for  $l_i$ . Note this formula suits for both conv and pool layers.

Since the output feature size of all sink vertices of  $\mathcal{M}$  is given (corresponding to  $\mathcal{F}^k$ ), we can iteratively calculate all the output and input feature size of all layers in  $\mathcal{M}$  with a top-down algorithm. The input feature size of all the sources vertices of  $\mathcal{M}$  is the input feature size needed by device  $d_k$ .

##### 3.2.2 Inference Cost Of Devices

We use  $f(l_i; F_i^k)$  to denote the required floating operations (FLOPs) of conv layer  $l_i$  when generates an output feature map  $F_i^k$  with size  $c_i \times w_i \times h_i$ . Assume layer  $l_i$  is a conv layer with  $c_i' \times k_i^w \times k_i^h$  kernel size,  $c_i'$  output channel and  $s_i$  stride size. Since each floating scalar in the output feature is calculated by sliding the kernel over the input feature,  $f(l_i; F_i^k)$  can be given by:

$$f(l_i; F_i^k) = k_i^w k_i^h c_i' w_i h_i c_i. \quad (4)$$

Here we ignore the pool layers since they require far fewer FLOPs than conv layers (In Fig. 2).

Note the  $w_i$  and  $h_i$  in Eq. (3) denote the region of correct output feature. However, the  $F_i^k$  is the actual output feature size, which contains not only the correct output but also some redundant part at the margin of  $F_i^k$ . Assume the size

of  $F_i^k$  is known and  $(l_i, l_j)$  is an edge in  $\mathcal{M}$ , the output  $F_j^k$  of layer  $l_j$  can be calculated by:

$$w_j = \frac{w_i + 2p_j^w - k_j^w}{s_j^w} + 1, \quad h_j = \frac{h_i + 2p_j^h - k_j^h}{s_j^h} + 1 \quad (5)$$

where  $p_j^w$  and  $p_j^h$  is the padding size of conv layer  $l_j$ . Since we have the input feature size for all source vertices in  $\mathcal{M}$ , to calculate the  $F_i^k$  for all layer  $l_i \in \mathcal{M}$ , we use a bottom-up algorithm similar with above, omit here.

So far if a device  $d_k$  is responsible to produce  $\mathcal{F}^k$  with model segment  $\mathcal{M}$ , we can give the required FLOPs operation  $\theta(\mathcal{M}; \mathcal{F}^k)$  with:

$$\theta(\mathcal{M}; \mathcal{F}^k) = \sum_{l_j \in \mathcal{M}} f(l_j; F_j^k). \quad (6)$$

And the inference time  $t_{comp}(d_k, F_k)$  for device  $d_k$  can be estimated by the following equation:

$$t_{comp}(d_k, \mathcal{F}^k) = \alpha_k \frac{\theta(\mathcal{M}; \mathcal{F}^k)}{\vartheta(d_k)} \quad (7)$$

where  $\vartheta(d_k)$  is the computing capacity (FLOPS) of device  $d_k$ .  $\alpha_k$  is a coefficient computed by a regression model.

### 3.2.3 The Period and Latency Of Pipeline

As each device executes inference in parallel within stage, the computation time for stage  $\mathcal{S} : \langle \mathcal{M}, \mathcal{D} \rangle$  is determined by the maximum inference time among devices in  $\mathcal{D}$ :

$$T_{comp}(\mathcal{S}) = \max_{d_k \in \mathcal{D}} t_{comp}(d_k, \mathcal{F}^k). \quad (8)$$

Since each device  $d_k \in \mathcal{D}$  will generate part of the calculation of stage  $\mathcal{S}$ , there exists a device  $d_f$  which is responsible to distribute stage input and gather stage output from other devices. For a device  $d_k \in \mathcal{S}$ , the feature transferring time  $t_{comm}(d_f, d_k, \mathcal{M})$  can be given by:

$$t_{comm}(d_f, d_k, \mathcal{F}) = \frac{\varphi(\mathcal{F}_{in}^k) + \varphi(\mathcal{F}_{out}^k)}{b} \quad (9)$$

where  $\varphi(\mathcal{F})$  is the feature size on a given input feature sizes  $\mathcal{F}$ . Here we use  $\mathcal{F}_{in}^k$  and  $\mathcal{F}_{out}^k$  to denote the input and output feature sizes of  $\mathcal{M}$  owned by  $d_k$ . Sum the communication cost for each device  $d_k$  in stage  $\mathcal{S}$ , we define

$$T_{comm}(\mathcal{S}) = \sum_{\substack{d_k \in \mathcal{D} \\ F_k \in \mathcal{F}}} t_{comm}(d_f, d_k, \mathcal{F}) \quad (10)$$

as the communication cost of stage  $\mathcal{S}$ .

The cost function for each stage in pipeline inference is then defined as the total time of the frame transfer and layer computation:

$$T(\mathcal{S}) = T_{comp}(\mathcal{S}) + T_{comm}(\mathcal{S}) \quad (11)$$

Note the time for feature map partition and stitch is not discussed here. In practice, it is far less than the layer computation time  $T_{comm}(\mathcal{S})$  and could be ignored.

Next we define the optimization objective as:

$$\mathcal{P}(\mathbb{G}, \mathbb{D}, \mathbb{S}) = \max_{\mathbb{S} \in \mathbb{S}} T(\mathcal{S}), \quad \mathcal{T}(\mathbb{G}, \mathbb{D}, \mathbb{S}) = \sum_{\mathbb{S} \in \mathbb{S}} T(\mathcal{S}) \quad (12)$$

where  $\mathcal{P}(\mathbb{G}, \mathbb{D}, \mathbb{S})$ ,  $\mathcal{T}(\mathbb{G}, \mathbb{D}, \mathbb{S})$  estimate the maximum execution time of stages in and inference latency in pipeline.

TABLE 1: Optimization Complexity

Device \ Model	Chain	Block	Graph
Homogeneous	P	NP*	NP
Heterogeneous	NP	NP	NP

\* [6] solves the optimization by considering entire block as a special layer. However, this operation introduces lots of unnecessary calculation during inference.

### 3.3 Analysis

The goal of our optimization algorithm is finding the best stage set  $\mathbb{S}^*$  that minimizes the maximum period  $\mathcal{P}(\mathbb{G}, \mathbb{D}, \mathbb{S})$  of pipeline with heterogeneous clusters. Such an optimization faces the following challenges:

- The overhead of computation and communication of each layer in model varies and would be affected by the assigned feature map size  $F_i^k$ .
- The computing capacity  $\vartheta(d_k)$  of every device in the heterogeneous cluster varies.
- For a specific stage  $\mathcal{S}$ , the number of devices  $|\mathcal{D}|$  and the model segment  $\mathcal{M}$  in stage also need to be configured.
- The structure of CNN model can be complex and hard to be partitioned.

In fact, we show the optimal solution can not be found in polynomial time unless  $P = NP$ .

**Theorem 1.** Given a CNN model  $\mathbb{G}$  with chain structure, the problem of minimizing maximum stage execution time  $\mathcal{P}(\mathbb{G}, \mathbb{D}, \mathbb{S})$  with heterogeneous mobile devices under a constriction that  $\mathcal{T}(\mathbb{G}, \mathbb{D}, \mathbb{S}) \leq T_{lim}$  is NP-hard.

**Proof 3.1.** Considering a scheduling problem defined as follows: Given  $L$  identical tasks that are needed to be executed one by one. All tasks can be paralleled to several processors without additional overhead. The goal is to assign these tasks to  $D$  heterogeneous devices and maximize the throughput. This problem is proven to be NP-hard by [16]. We can construct a CNN model with chain structure whose layers are identical and the kernel size of each layer is  $1 \times 1$ . This kernel size guarantees there is no overlapped partition when parallels the inference. If there exists a polynomial solution for this CNN model, obviously it can also be applied for the above task assignment problem. Thus, the optimization of  $\mathcal{P}(\mathbb{G}, \mathbb{D}, \mathbb{S})$  is NP-hard. Here complete the proof.

**Theorem 2.** Given a CNN model  $\mathbb{G}$  with graph structure, the problem of minimizing maximum stage execution time  $\mathcal{P}(\mathbb{G}, \mathbb{D}, \mathbb{S})$  with homogeneous mobile devices under a constriction that  $\mathcal{T}(\mathbb{G}, \mathbb{D}, \mathbb{S}) \leq T_{lim}$  is NP-hard.

**Proof 3.2.** We begin with introducing the problem of most balanced *st*-edge cuts (MBSTC). Given a graph  $G$ , founding an edge cut  $[G, \bar{G}]$ , which minimize  $\max\{|G|, |\bar{G}|\}$  is NP-Hard [17]. Obviously MBSTC is a special case of our optimization when the number of stages is 2. Thus, the problem is NP-Hard.

Given a heterogeneous edge environment, Theorem 1 shows find the optimal solution for CNNs with chain structure is NP-Hard. Theorem 2 shows that for CNNs with

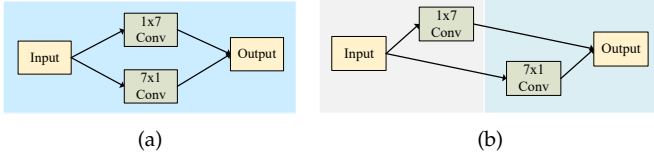


Fig. 6: A extreme case for a block with two layers. (a): consider entire block as a special layer. (b): partition the block into more fine-grained pieces.

graph structure, even homogeneous edge environment is NP-Hard.

We summarize the result in Table 1, almost every situation is NP-Hard for optimization except chain structure model with homogeneous devices.

## 4 ORCHESTRATE THE MODEL STRUCTURE

In this section, we introduce our strategy to orchestrate the complex block and graph structures.

### 4.1 Insight

Ideally, we hope to directly divide CNN model  $\mathbb{G}$  and mobile devices  $\mathbb{D}$  into several stages  $\mathbb{S}$ . However, we can find there is no polynomial solution for  $\mathbb{G}$  with block and graph structures from Table 1, neither with homogeneous nor heterogeneous environment. The only feasible situation to find the optimal strategy  $\mathbb{S}$  is that the structure of model is a chain.

For block structure, a simple trade-off is to consider every block as a special layer. So that it could be optimized in polynomial time. However, this scheme introduces lots of redundant calculation inside blocks and can not be applied on these models with graph structures. Fig. 6 shows an extreme case for such a scheme. Considering a block with only two conv layers ( $l_a, l_b$ ). The kernel size of  $l_a$  is  $1 \times 7$  but the kernel size of  $l_b$  is  $7 \times 1$ . For layer  $l_a$ , according to Eq. (3) there is no redundant calculation on its width dimension since  $k_a^w = 1$  (assuming the stride size is 1). Similarly, there is no redundant calculation on its length dimension for layer  $l_b$ . However, if we regard the block as a special whole layer, it will have redundant calculation on both width and length, as shown in Fig. 6a. But the block can be divided into two sequential *pieces*, one piece contains the input vertex and layer  $l_a$ , the other piece contains layer  $l_b$  and output vertex as shown in Fig. 6b. After this operation, there is no more redundant calculation inside the two pieces.

Here comes the insight. Given a CNN model  $\mathbb{G}$ , the goal is to transform it into a sequence of pieces. Since there may be some redundant calculation inside pieces, we need to minimize the redundancy inside every piece. After this operation, each piece can be regarded as a layer of original  $\mathbb{G}$ . Since these pieces construct a chain structure, the operation gives change for further optimization.

### 4.2 Partition Graph Into Pieces

We give a graph partition algorithm based on dynamic programming.

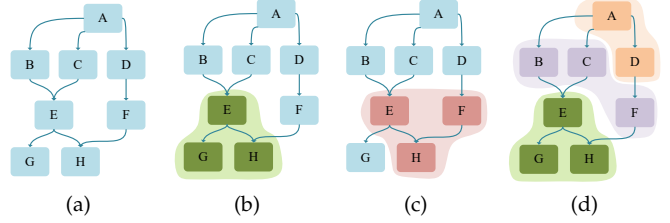


Fig. 7: The illustration of ending pieces. (a): The original graph  $\mathbb{G}$ . (b):  $\{E, G, H\}$  is an ending piece of  $\mathbb{G}$ . (c):  $\{E, F, H\}$  is not an ending piece of  $\mathbb{G}$ . (d): A partition of  $\mathbb{G}$  using ending piece iteratively.

Here we will reveal the existence of the optimal substructure property of the problem of partitioning graph into pieces, which is necessary for dynamic programming. We first define the concept of *ending piece* of graph  $\mathbb{G}$ . Note since the piece of  $\mathbb{G}$  is just a *smaller segment* defined in the previous section, we still use the notation  $\mathcal{M}$  to denote these pieces.

**Definition 4.** An *ending piece*  $\mathcal{M}_E$  is a special piece of  $\mathbb{G}$  which for any edge  $(u, v) \in \mathbb{G}$ , if  $u \in \mathcal{M}_E$ , then  $v \in \mathcal{M}_E$ .

The Fig. 7 gives an illustration of ending pieces. We plot a small graph  $\mathbb{G}$  with 8 vertices in Fig. 7a and two different pieces in Fig. 7b and Fig. 7c. The green region  $\{E, G, H\}$  in Fig. 7b is an ending piece of original graph  $\mathbb{G}$ . But the red region  $\{E, F, H\}$  in Fig. 7c is not an ending piece since the edge  $E$  is a member of this piece but  $G$  is outside the red region. The graph  $\mathbb{G}$  can be partitioned into pieces using the concept of ending piece recursively. Given a graph  $\mathbb{G}$ , the sketch of the procedure is to find an ending piece  $\mathcal{M}_E$  and add it to the partition result (a sequence of pieces), then consider the rest part  $\mathbb{G} - \mathcal{M}_E$  as a new graph and repeat the previous procedure recursively. Fig. 7d shows a partition result of graph  $\mathbb{G}$ .

Note partition  $\mathbb{G}$  by ending piece can not guarantee that these pieces obtained are with a chain structure. If we assign vertex  $B$  in Fig. 7d from the middle piece  $\{B, C, F\}$  to the first piece  $\{A, D\}$ , the partition result can also be obtained by the above procedure. However, such a result do not satisfy our goal since the first piece connects with two pieces at the same time. To prevent this, we add a constraint that all the vertices that are directly connect to the ending piece must belong to the ending piece in the next iteration. With this constraint, once  $\{E, G, H\}$  is determined as ending piece,  $\{B, C, F\}$  must belong to the same piece in the final result, which guarantees the obtained pieces a chain structure.

### 4.3 The Algorithm

Since our goal to minimize the redundant calculation of every piece, we need to quantify the redundant calculation cost  $C(\mathcal{M})$  for a given piece  $\mathcal{M}$ . Assume  $\mathcal{I}$  is the original input feature sizes of sources nodes in  $\mathcal{M}$ , and  $\mathcal{I}'$  is the feature size with redundant parts that are calculated with Eq. (3). The value of  $C(\mathcal{M})$  can be easily quantified by the difference of required FLOPs for the two input.

**Algorithm 1** Partition graph into pieces

---

**Require:**  $F$ : map indexed with the hash  $h(\mathbb{G})$  and return  $F(\mathbb{G})$ .  
**Require:**  $R$ : map indexed with the hash  $h(\mathbb{G})$  and return  $\mathcal{M}$ .

- 1: **function** PARTITION( $\mathbb{G}, \mathcal{M}'_E$ )
- 2:   compute the hash  $h(\mathbb{G})$
- 3:   **if**  $F$  contains  $h(\mathbb{G})$  **then**  
       **return**  $F[h(\mathbb{G})]$
- 4:    $min \leftarrow \infty$
- 5:   get  $\mathcal{M} \subset h(\mathbb{G})$  which directly is connected with  $\mathcal{M}'_E$
- 6:   **for**  $\mathcal{M}_E \leftarrow DFS(\mathbb{G} - \mathcal{M})$  **do**
- 7:      $\mathcal{M}_E \leftarrow \mathcal{M}_E \cup \mathcal{M}$
- 8:     calculate the redundancy  $C(\mathcal{M}_E)$
- 9:      $cur \leftarrow \max(\text{partition}(\mathbb{G} - \mathcal{M}_E, \mathcal{M}_E), C(\mathcal{M}_E))$
- 10:    **if**  $min > cur$  **then**
- 11:      $F[h(\mathbb{G})] = cur$
- 12:      $R[h(\mathbb{G})] = \mathcal{M}_E$
- 13:      $min \leftarrow cur$
- 14:    **return**  $F[h(\mathbb{G})]$
- 15: **function** OBTAIN( $\mathbb{G}$ )
- 16:   **if**  $\mathbb{G} == \phi$  **then**  
       **return**
- 17:    $\mathcal{M} \leftarrow R[h(\mathbb{G})]$
- 18:   print the piece  $\mathcal{M}$
- 19:   obtain( $\mathbb{G} - \mathcal{M}$ )

---

Here we give the state transfer equation for partitioning the graph structure:

$$F(\mathbb{G}) = \min_{\mathcal{M}_E \subset \mathbb{G}} \{\max\{F(\mathbb{G} - \mathcal{M}_E), C(\mathcal{M}_E)\}\}. \quad (13)$$

If  $\mathbb{G}$  is partitioned into multiple pieces  $\mathcal{M}$ , the function  $F(\mathbb{G})$  return the minimum FLOPs difference  $C(\mathcal{M})$  among all partitioned pieces in  $\mathbb{G}$ . Algorithm 1 gives the pseudocode.

**Line 2-4** checks whether  $F(\mathbb{G})$  is already calculated, if true, the following computation can be skipped. Otherwise, we use a variable  $min$  to store the minimum value that located in Eq. (13).

**Line 5-7** add a constraint to make sure the partitioned pieces following a chain structure. Since the *partition* function uses recursion, the parameter  $\mathcal{M}'_E$  stores the partitioned piece in its previous calculation. We use a *DFS* function to produce all the possible  $\mathcal{M}_E$ .

**Line 8-13** is the core part of our proposed dynamic programming. It iterates all possible  $\mathcal{M}_E$ , and uses recursion to solve the optimization problem. Here we use a variable  $cur$  to store the best partition strategy for current  $\mathcal{M}_E$ . If the current strategy is better than the one we have recorded, we update the record variable  $min$  and map  $F$  and  $R$ .

**Line 14-18** is the *obtain* function which receives the CNN  $\mathbb{G}$  and shows the best partition strategy using the map  $R$  that calculated in the *partition* function.

Note the *DFS* function can produce tons of available  $\mathcal{M}_E$  for a given  $\mathbb{G}$ . Since iterating all of them leads to unfeasible complexity for optimization, we use a simple pruning strategy here. From the above discussion, it is clear that the more sequential layers we fuse, the more redundancy we get. In fact, we observe that the redundancy is intolerable when the *diameter* of  $\mathcal{M}_E$  exceeds a specific number.

**Definition 5.** The diameter of piece  $\mathcal{M}$  is the greatest distance of any vertex pair in  $\mathcal{M}$ .

**Algorithm 2** Dynamic programming for pipeline inference

---

**Require:**  $P, L$ : 3D arrays used to record the period and latency.  
**Require:**  $S, R$ : 3D array used to trace the computed stage and sub-pipeline.

- 1: **function** DP( $i, j, p, T_{lim}$ )
- 2:   **if**  $P[i][j][p]$  exists **then**  
       **return**  $P[i][j][p], L[i][j][p]$
- 3:   calculate  $Ts[i][j][p]$  using (11)
- 4:    $P[i][j][p] \leftarrow Ts[i][j][p]$
- 5:    $T[i][j][p] \leftarrow Ts[i][j][p]$
- 6:    $S[i][j][p] \leftarrow (i, j, p)$
- 7:   **if**  $m = 1$  or  $j = i + 1$  **then**  
       **return**  $P[i][j][p], T[i][j][p]$
- 8:   **for**  $s := i \rightarrow j - 1$  **do**
- 9:     **for**  $m := 1 \rightarrow p - 1$  **do**
- 10:      calculate  $Ts[s + 1][j][m]$  using (11)
- 11:       $T_{lim} \leftarrow T_{lim} - Ts[s + 1][j][m]$
- 12:      **if**  $T_{lim} < 0$  **then**  
         **continue**
- 13:      **continue**
- 14:       $P[i][s][p - m], T[i][s][p - m] \leftarrow DP(i, s, p - m, T_{lim})$
- 15:      **if**  $T_{lim} < T[i][j][p - m]$  **then**  
         **continue**
- 16:      **continue**
- 17:       $period \leftarrow \max(P[i][s][p - m], Ts[s + 1][j][m])$
- 18:      **if**  $period < P[i][j][p]$  **then**
- 19:         $P[i][j][p] \leftarrow period$
- 20:         $T[i][j][p] \leftarrow T[i][s][p - m] + Ts[s + 1][j][m]$
- 21:         $R[i][j][p] \leftarrow (i, s, p - m)$
- 22:         $S[i][j][p] \leftarrow (s + 1, j, m)$
- 23:      **return**  $P[i][j][p], L[i][j][p]$
- 24: **function** BUILDSTRATEGY( $(i, j, p), \mathbb{S}$ )
- 25:   **if**  $R[i][j][p]$  **then**  
       BuildStrategy( $R[i][j][p], \mathbb{S}$ )
- 26:   calculate  $S_{i \rightarrow j}$  using  $S[i][j][p]$
- 27:    $\mathbb{S} \leftarrow S_{i \rightarrow j} \cup \mathbb{S}$

---

With this observation, we limit the diameter of produced  $\mathcal{M}_E$  in *DFS* function under a constant integer *dia*. In practice, we set the value of *dia* to 5.

## 5 PIPELINE COOPERATION FOR CNN INFERENCE

In this section, we present a pipeline cooperation (PICO) scheme aimed at efficiently executing CNN inference. PICO uses a heuristic algorithm based on dynamic programming to optimize the inference pipeline. We also implement an adaptive framework which automatically chooses suitable parallel scheme under dynamic workload.

### 5.1 Heuristic

For chain structure, although the polynomial algorithm for  $\mathcal{P}(\mathbb{G}, \mathbb{D}, \mathbb{S})$  does not exist unless  $P = NP$ , the optimal solution can be found in polynomial time if these mobile devices are homogeneous, which lead to a heuristic two-step algorithm. We first find the optimal  $\mathbb{S}^*$  for a homogeneous cluster, then adapt the  $\mathbb{S}^*$  to a heterogeneous cluster using a greedy algorithm.

Since the CNN  $\mathbb{G}$  is partitioned into  $L$  pieces, considering a specific stage  $\mathcal{S} : \langle \mathcal{M}, \mathcal{D}, \mathcal{F} \rangle$  that starts from  $i$ -th piece and ends at  $j$ -th piece. We can use the notation  $\mathcal{S}_{i \rightarrow j}$  to represent it, so to the two notations  $\mathcal{M}_{i \rightarrow j}$  and  $\mathcal{D}_{i \rightarrow j}$ .



### 5.1.1 Dynamic Programming

Given a cluster  $\mathbb{D}$ , we construct a new cluster  $\mathbb{D}'$ , which has the same number of devices of  $\mathbb{D}$ , but the computing capacity of each device is equivalent to the average of  $\mathbb{D}$ .

$$\vartheta(d'_k) = \frac{\sum_{d_k \in \mathbb{D}} \vartheta(d_k)}{|\mathbb{D}|} \quad \forall d'_k \in \mathbb{D}', \quad |\mathbb{D}'| = |\mathbb{D}| \quad (14)$$

For any device  $d_k$  belongs to this stage, the output feature size  $\mathcal{F}^k$  is equivalently partitioned. Thus,  $\mathcal{F}^k$  can be determined by the size of stage. We denote  $p = |\mathcal{D}_{i \rightarrow j}|$  for convenience.

The expression of stage can now be simplified as a three-element tuple  $(i, j, p)$ . For the optimal pipeline  $\mathbb{S}^*$ , it can now be broken into an optimal sub pipeline consisting of pieces form 1 through  $s$  with  $p - m$  mobile devices followed by a single stage with pieces  $s + 1$  through  $j$  replicated over  $m$  workers. Then using the optimal sub-problem property, we can solve the optimization problem through dynamic programming:

$$P[i][j][p] = \min_{i \leq s < j} \min_{1 \leq m < p} \max \left\{ \begin{array}{l} P[i][s][p - m] \\ T_s[s + 1][j][m] \end{array} \right. \quad (15)$$

where  $P[i][s][p - m]$  is the time taken by the slowest stage of the optimal sub-pipeline between piece  $i$  and  $s$  with  $p - m$  edge devices,  $T_s[s + 1][j][m]$  is the time taken for a stage with model segment  $\mathcal{M}_{s+1 \rightarrow j}$  with  $m$  devices. Obviously  $P[1][L][D]$  is equivalent to  $\mathcal{P}(\mathbb{G}, \mathbb{D}', \mathbb{S})$  in the homogeneous case. During optimization, we prune these solutions that exceed the inference limitation  $T_{lim}$ .

Algorithm 2 shows the pseudocode of our optimization algorithm which uses dynamic programming with memorization to find out the optimal parallelization strategy. Function  $DP$  computes the minimum period and records the optimal pipeline configuration in two 3D arrays  $R$  and  $S$ . The optimal parallelization strategy is built up through function  $BuildStrategy$  by recursively iterating the calculated  $R$  and  $S$ , and adding the corresponding stage configuration  $\mathcal{S}_{i \rightarrow j}$  to  $\mathbb{S}$ .

### 5.1.2 Adapt to the heterogeneity

We use a greedy algorithm to adapt the calculated  $\mathbb{S}'$  in Algorithm 2 to the heterogeneous environment. For every stage  $\mathcal{S}'_{i \rightarrow j} \in \mathbb{S}'$ , we keep the model segment  $\mathcal{M}_{i \rightarrow j}$  unchanged and choose a proper set of edge devices as  $\mathcal{D}_{i \rightarrow j}$  from heterogeneous cluster  $\mathbb{D}$ . Let  $\Theta_{i \rightarrow j}$  and  $\Theta'_{i \rightarrow j}$  denotes the required computing resources of stage  $\mathcal{S}_{i \rightarrow j}$  and  $\mathcal{S}'_{i \rightarrow j}$ :

$$\Theta_{i \rightarrow j} = \sum_{d_k \in \mathcal{D}_{i \rightarrow j}} \theta(\mathcal{M}_{i \rightarrow j}; \mathcal{F}^k), \quad (16)$$

We want  $\Theta_{i \rightarrow j}$  are as close to  $\Theta'_{i \rightarrow j}$  as possible.

We initialize the stage set  $\mathbb{S}$  with the same number of stages, each stage only the same number of workers and the same model fragment  $\mathcal{S}_{i \rightarrow j}$ . To achieve our goal, we sort the mobile devices by the computing capabilities  $\vartheta(d_k)$  in reverse order and then iterate each device. In every iteration, we find the stage  $\mathcal{S}'_{i \rightarrow j} \in \mathbb{S}'$  with maximum average computing requirement  $\frac{\Theta_{i \rightarrow j}}{|\mathcal{D}'_{i \rightarrow j}|}$ . The current device  $d_k$  will be added to device set  $\mathcal{D}_{i \rightarrow j}$ . Once  $\mathcal{D}_{i \rightarrow j}$  owns the same number of device in  $\mathcal{D}'_{i \rightarrow j}$ , we adjust the output feature

### Algorithm 3 Adjust stage configuration $\mathbb{S}$ for heterogeneous devices

**Require:**  $\mathbb{S}'$ : the optimal stage set for homogeneous cluster.

- 1: **function** ADJUSTSTAGE
- 2: Initialize an empty  $\mathbb{S}$
- 3: Sort devices in  $\mathbb{D}$  by compute capabilities  $\vartheta(d_k)$
- 4: **for**  $d_k \in \mathbb{D}$  **do**
- 5: Find the stage  $\mathcal{S}'_{i \rightarrow j} \in \mathbb{S}'$  with minimum  $\frac{\Theta'_{i \rightarrow j}}{|\mathcal{D}'_{i \rightarrow j}|}$
- 6: Get  $\mathcal{S}_{i \rightarrow j}$  from  $\mathbb{S}$  or create  $\mathcal{S}_{i \rightarrow j}$  with empty  $\mathcal{D}_{i \rightarrow j}$
- 7:  $\mathcal{D}_{i \rightarrow j} \leftarrow d_k \cup \mathcal{D}_{i \rightarrow j}$
- 8: Remove one device from  $\mathcal{D}'_{i \rightarrow j}$
- 9: **if**  $|\mathcal{D}'_{i \rightarrow j}| = 0$  **then**
- 10: Adjust feature partition  $\mathcal{F}^k$  for every  $d_k \in \mathcal{D}_{i \rightarrow j}$ .
- 11:  $\mathbb{S} \leftarrow \mathcal{S}_{i \rightarrow j} \cup \mathbb{S}$
- 12: Remove  $\mathcal{S}'_{i \rightarrow j}$  from  $\mathbb{S}'$

**return**  $\mathbb{S}$

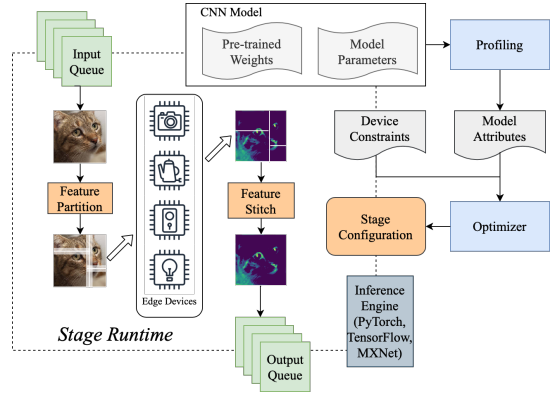


Fig. 8: The workflow of stages in an inference pipeline.

size  $\mathcal{F}^k$  for every device  $d_k \in \mathcal{D}_{i \rightarrow j}$  with a *Divide And Conquer* algorithm. After this operation, we accomplish the presentation of stage  $\mathcal{S}_{i \rightarrow j}$  and add it to  $\mathbb{S}$ . After all the iterations, we have a set of stages  $\mathbb{S}$  for the heterogeneous cluster. The complete algorithm is shown in Algorithm 3.

## 5.2 Implementation

**The workflow of stages:** We summarize the workflow of stages in Fig. 8. Each stage owns its configuration  $\mathcal{S}_{i \rightarrow j}$  which is given by the previous optimization. The main thread of stage takes the feature map from the input queue, then splits it into small tiles with different size according to  $\mathcal{F}$  and distributes them to those devices  $\mathcal{D}_{i \rightarrow j}$ . Once the computation finishes, the outputs of those devices is gathered and stitched together. There are two other threads responsible to put the receiving feature map into the input queue and to send the output to the next stage.

**Feature split and stitch:** Most popular DL framework such as TensorFlow, PyTorch does not provide an efficient way to split feature map with overlapped parts, and use these high level provided by those frameworks to implement the operations brings intolerable latency. We accomplish the frame split and stitch operations by directly operate the frame tensor data point in the memory space through C++. In practice, after optimization, the time consumption of feature split and stitch can be ignored.

**Represent CNN into graph:** We implement an automatic *GraphConverter* module to convert a given CNN model file



Fig. 9: The testbed in our experiment composed by 8 Raspberry-Pi 4Bs and one Wi-Fi access point.

into a DAG. The module will record the input and output layer for every tensor during profiling. To achieve this, We modify the source file of PyTorch and add a new hook function `register_prev_forward_hook` as suggested in [18].

## 6 EXPERIMENT

We give the details of our evaluation bed for experiment and analyze the obtained result.

### 6.1 Environment Setup

Here we give the details of our evaluation setup.

**Hardware:** The mobile cluster for evaluating the PICO framework uses one Wi-Fi access point with 50Mbps bandwidth and 8 ARM based Raspberry-Pi 4Bs. Each Raspberry-Pi 4B has a Quad Core ARM Cortex-A73, which has 1.5 GHz max CPU frequency. It has 2 GB LPDDR2 SDRAM, and dual-band 2.4 GHz/5 GHz wireless for communication. To represent a realistic low-end mobile device cluster, we set these Raspberry-Pi 4B running with one CPU core during inference. Fig. 9 shows the test bed we used, the laptop is used to monitor and control this cluster.

**Models overview:** VGG16 [12] is a classic CNN classification model. It contains 13 conv layers, 5 pooling layers and 3 fc layers. You only look once version 2 (YOLOv2) [13] is a lightweight CNN used for real-time object detection system. It has deeper architecture compared with VGG-16. There are 23 conv and 5 pooling layers in YOLOv2, nearly twice of VGG16. Both VGG16 and YOLOv2 follow the chain structure. ResNet34 [10] and InceptionV3 [11] are two classic CNNs that use a block structure. ResNet34 uses a *skip-connection* strategy that allow the feature to skip several layers. Compared with ResNet34, InceptionV3 have more complex structure. The Inception block has multiple branches, and the conv layers also have many unbalanced (e.g.,  $1 \times 7$ ,  $5 \times 1$ ) kernels.

**Compared method:** For VGG16 and YOLOv2, four different parallelization strategies are used the evaluation: (1) Layer-wise (LW) scheme, which parallelizes the CNNs layer by layer; (2) Early-fused-layer (EFL) scheme, an extension to the implementation of DeepThings [5], which fuses and parallelizes the first few conv layers, then executes the rest layers in a single device; (3) Optimal Fused-layer (OFL)

scheme, which selectively fuses convolution layers at different parts of a model; (4) Pipeline Cooperation (PICO) scheme, which is proposed in this paper. For ResNet34 and YOLOv2, we compare two different graph partition strategy: (1) Consider each block as a piece, which is used in [6]. (2) Partition the entire graph into multiple pieces, which is proposed in this paper.

### 6.2 Pipeline Performance

We evaluate a bunch of metrics of our proposed pipeline cooperation scheme.

**Maximum throughput:** Fig. 10 and Fig. 11 plot the cluster capacity when executing VGG16 and YOLOv2 with different parallel schemes. The first three figures plot the inference period with different parallel schemes and CPU frequencies. The last figure plots the accomplished inference task per minute with 8 devices. It represents the throughput of different parallel schemes. PICO has the best performance as expected, since our optimization goal is to reduce the redundant computation and achieve minimum pipeline period. When the number of devices increases, the throughput of different strategies also improve except the executing YOLOv2 using layer-wise scheme with 1GHz CPU core. YOLOv2 has nearly twice number of layers compared with VGG16, which brings more communication overhead for Layer-wise strategy. When the computing resource is rich (1GHz), the gain brought by the increasing number of devices is offset by communication overhead. Early-fused-layer and optimal-fused-layer schemes fuse multiple layers into one model segment, and do not require communication among devices when they are executing one segment, thus the communication overhead is reduced. Since optimal-fused-layer scheme optimizes the configuration of fused layers, it outperforms early-fused-layer which simply fuses the very early layers. However, when the number of devices is bigger than a certain number(4 for example), the improvement is very tiny due to the additional computation CPU redundancy.

**Different Memory Footprint:** We use a python script to sample memory footprint from `/proc/pid/status` for each inference process. Fig. 12 plots the average memory footprint of different algorithms. According to our previous discussion, the memory footprint can be divided into three more fine-grained parts. The *Model* and *Feature* denote how much the model parameters and intermediate features take part in the memory footprint. Additionally, we also plot the basic memory footprint (*Base*) of inference framework to give a more practical meaning to the real world application. We can find the memory footprint decreases as the number of mobile devices increases. Since LW, FL, DFL only split features, the whole model need to be replicated on all mobile devices. This approach leads to a result that they can only decrease the memory footprint caused by intermediate features. Meanwhile, PICO distributes both model and features, thus reduces the memory footprint obviously, especially in Fig. 12b as YOLOv2 owns more conv layers and model parameters than VGG16. And we have an interest discovery. The LW algorithm use less memory comparing with FL and DFL in Fig. 12a, which satisfies our assumption since LW has the least redundancy during feature stitch. But

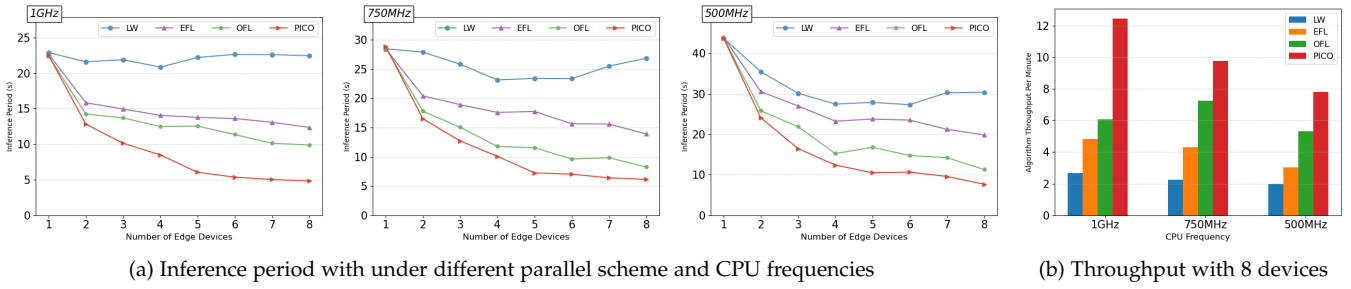


Fig. 10: The cluster capacity when executing VGG16.

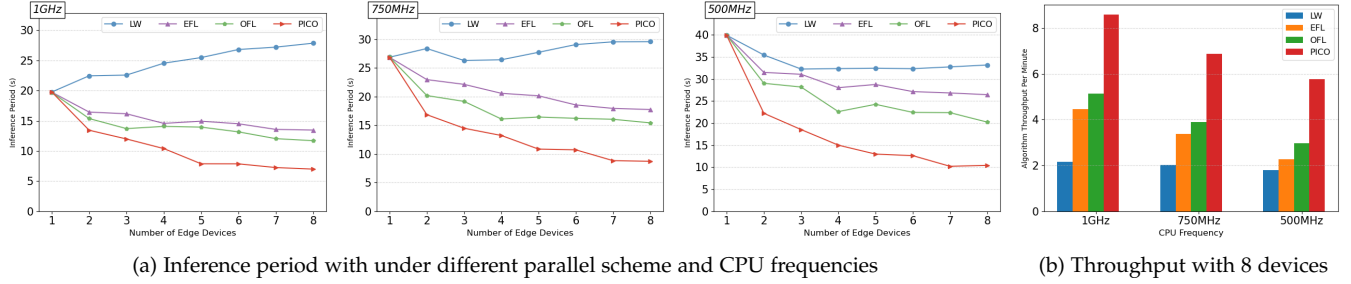


Fig. 11: The cluster capacity when executing YOLOv2.

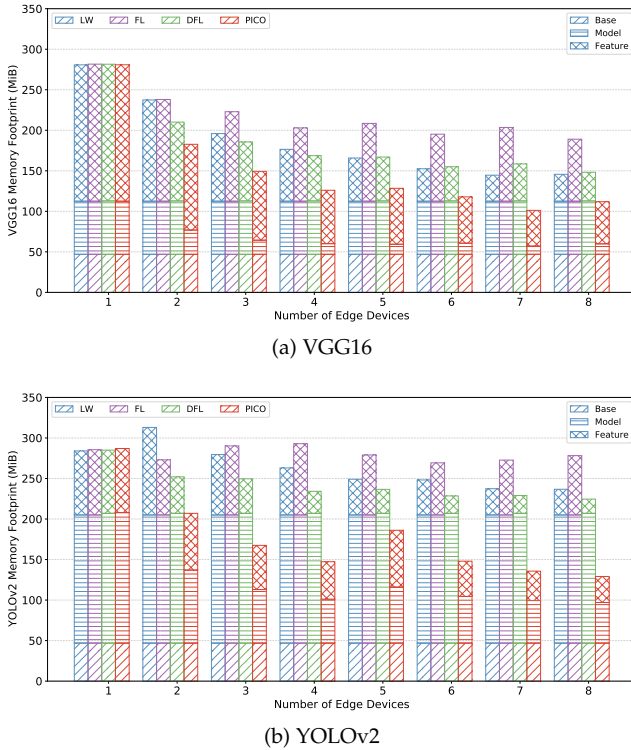


Fig. 12: The memory footprints of these algorithms

in Fig. 12b, LW performs not that good, when using 2 mobile devices, the average memory footprint is even larger than using single devices. According to Table 2, we can find the first device use a lot of memory than others do. The reason is that the first device need to communicate with others and is in charge of splitting and stitching features as suggested

in [4]. Since YOLOv2 owns twice times layers than VGG16, these operations raises the problem.

**Resource utilization:** We monitor the CPU usage during inference on a heterogeneous edge cluster and record the average computing resource utilization ratio (Utili.) for different parallel scheme. We also calculate the redundancy ratio (Redu.) during computation. The result is presented in Table 2. With the greedy algorithm 3, the PICO can adjust the proper partition size for each device, thus the resource utilization of different heterogeneous devices keeps at a high level (77.18% and 94.89% for VGG16 and YOLOv2). In the same time, the redundant computation is kept in low percentages. Layer-wise scheme has the minimum average redundant computation but also has the worst performance on resource utilization. Those fused-layer schemes keep the devices busy, but many computations are redundant. Especially for the early-fused-layer scheme which has 46.54% percent redundancies executing YOLOv2. Through optimal-fused-layer scheme optimizes the configuration, the redundancy ratio is still higher than PICO since PICO uses a subset of mobile devices instead of the entire cluster.

### 6.3 Graph Partition

Here we present some experimental result of our proposed graph partition algorithm.

**Details about partitioned pieces:** The Fig. 13 shows part of the partition result of InceptionV3 model. The Fig. 13a plots the InceptionC block, which consists 4 branches and 10 neural layers. We can find if we consider entire block as a layer [6], lots of redundant calculation will be introduced since there are many *unbalanced* conv kernel (e.g.,  $1 \times 7$  and  $7 \times 1$ ). We can use Eq. (3) and Eq. (5) to quantify the redundant calculation. If we fuse entire block into one pieces (used in [6]), the devices have to

TABLE 2: The utilization, redundancy ratios and memory footnotes with different parallel schemes.

Model	Attributes	Methods	Type	Devices								Average
				1.2GHz	1.2GHz	800MHz	800MHz	600MHz	600MHz	600MHz	600MHz	
VGG16	Layers: 13 conv + 5 pool  Input size: 244 × 244	LW	Utili	30.35%	23.66%	32.41%	32.64%	44.08%	45.85%	43.50%	44.99%	37.19%
			Redu	2.35%	2.35%	1.82%	1.82%	1.93%	1.93%	2.23%	2.23%	2.08%
			Mem	210.0 M	142.0 M	146.0 M	142.3 M	144.0 M	143.0 M	148.2 M	146.2 M	152.7 M
		EFL	Utili	33.64%	34.87%	74.19%	76.76%	95.96%	98.63%	66.77%	66.86%	68.46%
			Redu	13.54%	14.14%	22.78%	23.66%	22.28%	23.10%	15.07%	15.75%	18.79%
			Mem	156.0 M	159.0 M	183.0 M	193.0 M	187.0 M	197.0 M	162.6 M	179.0 M	177.1 M
		OFL	Utili	40.30%	41.58%	62.79%	63.79%	88.31%	97.08%	79.27%	83.07%	69.53%
			Redu	8.77%	8.99%	12.91%	13.18%	12.14%	12.35%	9.62%	9.78%	10.97%
			Mem	153.0 M	153.0 M	163.0 M	164.0 M	159.6 M	160.0 M	156.0 M	157.5 M	158.3 M
		PICO	Ratio	96.49%	95.46%	79.03%	77.61%	64.77%	40.76%	70.67%	92.65%	77.18%
Redu	10.44%		10.33%	5.22%	0.00%	6.33%	4.95%	3.22%	3.22%	5.47%		
Mem	252.0 M		147.0 M	124.0 M	106.0 M	94.0 M	124.0 M	118.0 M	114.0 M	134.8 M		
YOLOv2	Layers: 23 conv + 5 pool  Input size: 448 × 448	LW	Utili	26.77%	22.55%	29.50%	29.39%	45.66%	45.11%	44.74%	44.07%	35.97%
			Redu	0.54%	0.54%	1.07%	1.07%	0.95%	0.95%	0.66%	0.66%	0.80%
			Mem	334.0 M	233.0 M	227.0 M	227.0 M	233.0 M	232.0 M	232.0 M	232.0 M	243.2 M
		EFL	Utili	37.85%	35.64%	67.24%	67.61%	96.01%	95.28%	75.87%	72.81%	68.54%
			Redu	27.09%	27.09%	45.08%	45.08%	44.68%	44.68%	29.29%	29.29%	36.54%
			Mem	189.0 M	178.0 M	208.0 M	208.0 M	208.0 M	207.0 M	178.0 M	178.0 M	194.2 M
		OFL	Utili	47.34%	47.96%	71.59%	70.87%	95.32%	94.98%	87.31%	87.61%	75.37%
			Redu	11.14%	11.14%	13.02%	13.02%	14.53%	14.53%	9.64%	9.64%	12.08%
			Mem	232.0 M	229.0 M	232.0 M	232.0 M	232.0 M	232.0 M	232.0 M	232.0 M	231.6 M
		PICO	Utili	88.01%	96.84%	88.50%	96.75%	99.00%	98.96%	90.97%	98.30%	94.89%
Redu	8.30%		0.00%	3.48%	13.27%	13.27%	7.89%	8.17%	6.76%	7.64%		
Mem	202.0 M		132.0 M	105.0 M	113.0 M	110.0 M	119.0 M	155.0 M	153.0 M	136.1 M		

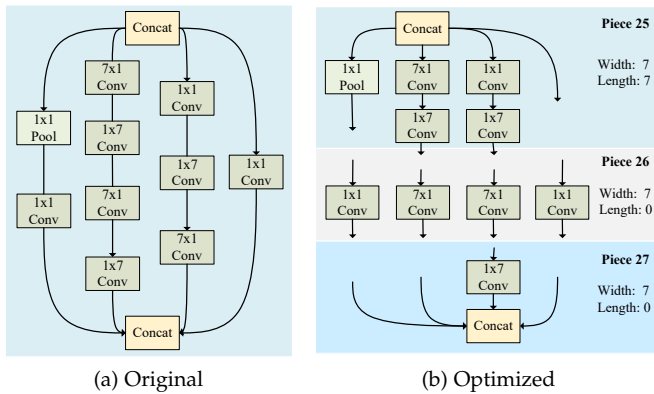


Fig. 13: An illustration of our graph partition algorithm. (a) Part of InceptionV3 model (InceptionC block). (b) The obtained pieces after optimization.

introduce 13 pixel length on both the width and height dimension. After running the partition algorithm, the block is split into three pieces (Piece 25, Piece 26 and Piece 27) as shown in Fig. 13b (The full partition result is attached in the supplemental material). The entire InceptionV3 model is composed with 40 pieces, but due to the size of model, we can not plot the entire model here. The complete partition result is shown in the supplemental materials. These pieces have much smaller redundant calculation. Piece 25 has 7 pixel length redundancy, and Piece 26 and Piece 27 only have redundancy on only one dimension. Compared with Fig. 13a, the redundant calculation during inference can be significantly reduced. In addition, since we break block into

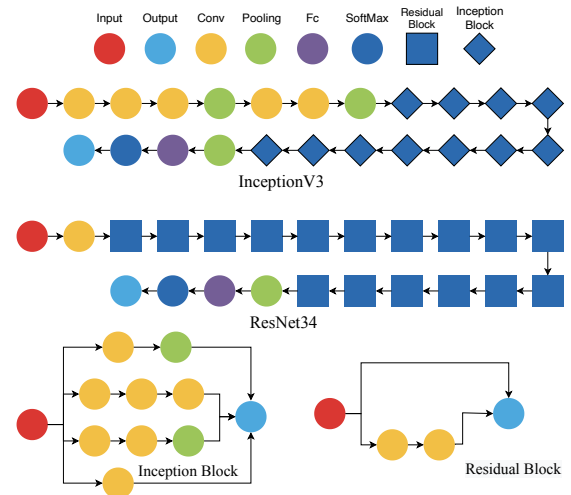


Fig. 14: The model structure of ResNet34 and InceptionV3.

pieces, the later optimization can make more fine-grained optimization.

**Speedup for CNNs with non-chain structure:** We can adapt PICO to those CNNs with non-chain structure by applying our graph partition algorithm at first. Here we compare the speedup ratio for ResNet34 and InceptionV3. Fig. 14 shows the structures of the two model, obviously they are constructed with the block structure. According to the figure we can find the Inception block in InceptionV3 is more complex than Residual block used in ResNet34. Fig. 15 plot the speedup ratio under different CPU frequencies for ResNet34 and InceptionV3 with different strategy. The figures on the left part fuse the entire block into a whole,

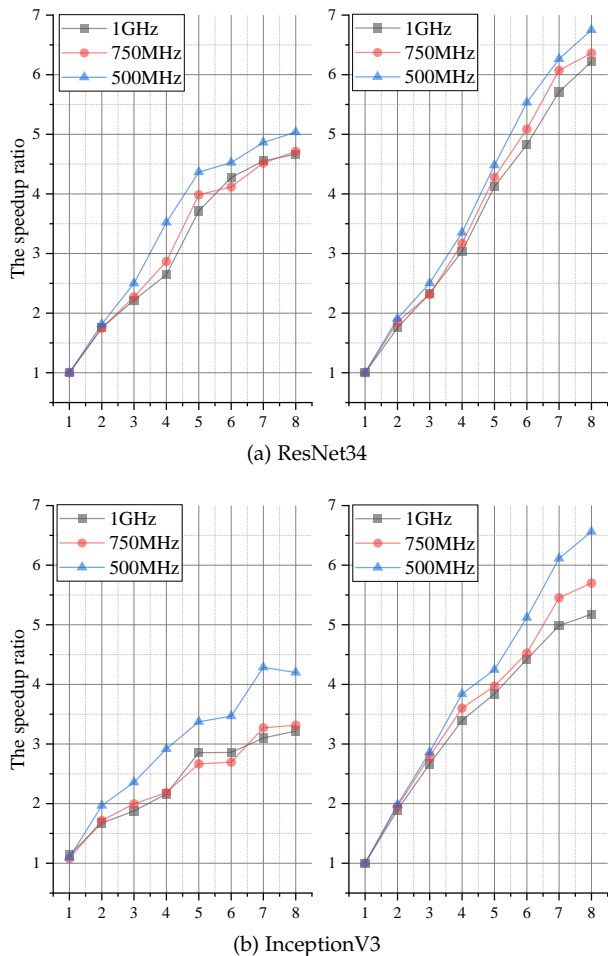


Fig. 15: The speedup ratio for ResNet34 and InceptionV3. The left part shows the result by treating entire block as a whole, and the right part uses graph partition algorithm.

and the figures on the right show the results that adopt our graph partition algorithm. When executing CNN inference with 8 devices, PICO can achieve  $6.8\times$  speedup for ResNet34 and  $6.5\times$  for InceptionV3 after partitioning the CNN model. The speedup effect is more obvious with low CPU frequency since the limitation of computing resource is relieved when the number of mobile devices increases. As for the strategy of fusing the entire block, it achieves up to  $5\times$  speedup for ResNet34, but only  $4\times$  for InceptionV3 when the CPU frequency is low. We think it is caused by the difference of the number of layers in Residual and Inception blocks. Since the Inception block contains more layers than Residual block, the optimal model partition is more likely to exist within blocks.

## 7 RELATED WORK

Along with the problem of enabling DNN-based intelligent applications, previous researches can be divided into two categories.

**Inference offloading:** Due to the limited up-link of mobile devices, traditional way of uploading captured data to the cloud server is time-consuming [19], [20]. Researchers focus on offloading the computation of early layers to mobile devices (*Inference offloading*). To minimize the inference

latency, Neurosurgeon [21] proposed to partition model between cloud server and mobile device according to the network situation. But [21] can only handle models with the chain structure. DADS [22] proposed a novel algorithm to partition DNN with graph structure using a min-cut algorithm. QDMP [23] noticed that directly applying min-cut on entire graph is time-consuming. Based on the block structure, [23] proposed a divide and conquer algorithm to find the min-cut, which achieves a nearly linear complexity in their experiments. Meanwhile, Branchynet [24] propose *early exit* mechanism by adding exit layers at the middle of DNN. This mechanism enables mobile device not feature map to cloud server if the local accuracy already reaches a certain value. Considering the situation when server does not have the corresponding model, IoNN [25] an incremental offloading technology which significantly improves the inference performance.

**Cooperative inference:** Recently researchers began to turn their attentions on executing inference completely at the edge with multiple mobile devices [4], [5], [6], [26]. MoDNN [4] is the first work in this field. MoDNN considers such a situation where several mobile devices cooperative inference under a Wi-Fi access point using layer wise strategy. In their following up work MeDNN [27], they used an adaptive feature map partition method according to the heterogeneous devices. Deepthings [5] proposed to fuse the early layers of DNNs. Note that the feature map between layers are partitioned horizontally in [4], [27], whereas Deepthings partitions the feature map into 2D grids to further reduce memory overhead. This method reduced the communication overhead, but increased the redundancy calculation. AOFL [6] use a dynamic programming based algorithm to find a trade-off between communication overhead and computation redundancy. For CNNs with block structure, [6] fused entire block into a whole, which introduces additional redundancy. [28] discussed using pipeline inference to achieve maximum throughput. But they only consider scheduling the number of input samples since the DNN they considered is already split into model segments, and they do not mention the redundant computation when partitioning the feature map. In addition, no previous works have proposed a solution for cooperative inference to deal with CNNs with graph structure.

## 8 CONCLUSION

In this paper, we propose a pipeline cooperation scheme (PICO) for efficiently executing inference with versatile CNN models and diverse mobile devices. This scheme improves the inference efficiency by reducing the redundant calculation. We first analyze the problem of partitioning CNNs and mobile devices into an inference pipeline. Using the analysis result, PICO uses a two-step strategy to build the pipeline. First, we orchestrate the graph structure of given CNN into a sequence of pieces. Then we divide these pieces and devices into several stages. The input data is fed into the first stage and the inference result is produced at the last stage. These stages compose an inference pipeline. We adjust the partition size of features among devices according to their computing resources. The execution time of each

stage is optimized to be as close as possible to gain maximum throughput. In our experiment with 8 RaspberryPi devices, the throughput can be improved by  $1.8 \sim 6.8\times$  under various settings.

## REFERENCES

- [1] G. Kour and R. Saabne, "Real-time segmentation of on-line handwritten arabic script," in *Frontiers in Handwriting Recognition (ICFHR)*. IEEE, 2014.
- [2] —, "Fast classification of handwritten on-line arabic characters," in *Soft Computing and Pattern Recognition (SoCPaR)*. IEEE, 2014.
- [3] Z. Zhou, X. Chen, E. Li, L. Zeng, K. Luo, and J. Zhang, "Edge intelligence: Paving the last mile of artificial intelligence with edge computing," *Proceedings of the IEEE*, 2019.
- [4] J. Mao, X. Chen, K. W. Nixon, C. Krieger, and Y. Chen, "Modnn: Local distributed mobile computing system for deep neural network," in *Design, Automation & Test in Europe Conference & Exhibition (DATE)*. IEEE, 2017.
- [5] Z. Zhao, K. M. Barijough, and A. Gerstlauer, "Deepthings: Distributed adaptive deep learning inference on resource-constrained iot edge clusters," *IEEE Transactions on Computer-Aided Design of Integrated Circuits and Systems*, 2018.
- [6] L. Zhou, M. H. Samavatian, A. Bacha, S. Majumdar, and R. Teodorescu, "Adaptive parallel execution of deep neural networks on heterogeneous edge devices," in *Proceedings of the 4th ACM/IEEE Symposium on Edge Computing*, 2019.
- [7] J. Li, Q. Qi, J. Wang, C. Ge, Y. Li, Z. Yue, and H. Sun, "Oicsr: Out-in-channel sparsity regularization for compact deep neural networks," in *Proceedings of the IEEE Conference on Computer Vision and Pattern Recognition*, 2019.
- [8] Y. He, P. Liu, Z. Wang, Z. Hu, and Y. Yang, "Filter pruning via geometric median for deep convolutional neural networks acceleration," in *Proceedings of the IEEE International Conference on Computer Vision*, 2019.
- [9] A. Howard, M. Sandler, G. Chu, L.-C. Chen, B. Chen, M. Tan, W. Wang, Y. Zhu, R. Pang, V. Vasudevan *et al.*, "Searching for mobilenetv3," in *Proceedings of the IEEE International Conference on Computer Vision*, 2019.
- [10] K. He, X. Zhang, S. Ren, and J. Sun, "Deep residual learning for image recognition," in *IEEE conference on computer vision and pattern recognition (CVPR)*, 2016.
- [11] C. Szegedy, S. Ioffe, V. Vanhoucke, and A. Alemi, "Inception-v4, inception-resnet and the impact of residual connections on learning," in *AAAI*, 2017.
- [12] K. Simonyan and A. Zisserman, "Very deep convolutional networks for large-scale image recognition," *arXiv preprint arXiv:1409.1556*, 2014.
- [13] J. Redmon and A. Farhadi, "Yolo9000: better, faster, stronger," in *Proceedings of the IEEE conference on computer vision and pattern recognition*, 2017.
- [14] B. Zoph, V. Vasudevan, J. Shlens, and Q. V. Le, "Learning transferable architectures for scalable image recognition," in *Proceedings of the IEEE conference on computer vision and pattern recognition*, 2018, pp. 8697–8710.
- [15] A. Benoit and Y. Robert, "Mapping pipeline skeletons onto heterogeneous platforms," *Journal of Parallel and Distributed Computing*, 2008.
- [16] —, "Complexity results for throughput and latency optimization of replicated and data-parallel workflows," *Algorithmica*, 2010.
- [17] P. Bonsma, "Most balanced minimum cuts," *Discrete Applied Mathematics*, vol. 158, no. 4, pp. 261–276, 2010.
- [18] A. Harlap, D. Narayanan, A. Phanishayee, V. Seshadri, G. R. Ganger, and P. B. Gibbons, "Pipedream: Pipeline parallelism for dnn training," in *Proceedings of the 1st Conference on Systems and Machine Learning (SysML)*, 2018.
- [19] J. H. Ko, T. Na, M. F. Amir, and S. Mukhopadhyay, "Edge-host partitioning of deep neural networks with feature space encoding for resource-constrained internet-of-things platforms," in *IEEE International Conference on Advanced Video and Signal Based Surveillance (AVSS)*. IEEE, 2018.
- [20] H. Li, C. Hu, J. Jiang, Z. Wang, Y. Wen, and W. Zhu, "Jalad: Joint accuracy-and latency-aware deep structure decoupling for edge-cloud execution," in *International Conference on Parallel and Distributed Systems (ICPADS)*, 2018.
- [21] Y. Kang, J. Hauswald, C. Gao, A. Rovinski, T. Mudge, J. Mars, and L. Tang, "Neurosurgeon: Collaborative intelligence between the cloud and mobile edge," *ACM SIGARCH Computer Architecture News*, 2017.
- [22] C. Hu, W. Bao, D. Wang, and F. Liu, "Dynamic adaptive dnn surgery for inference acceleration on the edge," in *IEEE International Conference on Computer Communications (INFOCOM)*. IEEE, 2017.
- [23] S. Zhang, Y. Li, X. Liu, S. Guo, W. Wang, J. Wang, B. Ding, and D. Wu, "Towards real-time cooperative deep inference over the cloud and edge end devices," *Proceedings of the ACM on Interactive, Mobile, Wearable and Ubiquitous Technologies*, 2020.
- [24] S. Teerapittayanon, B. McDanel, and H.-T. Kung, "Branchynet: Fast inference via early exiting from deep neural networks," in *International Conference on Pattern Recognition (ICPR)*, 2016.
- [25] H.-J. Jeong, H.-J. Lee, C. H. Shin, and S.-M. Moon, "Ionn: Incremental offloading of neural network computations from mobile devices to edge servers," in *ACM Symposium on Cloud Computing*, 2018.
- [26] R. Hadidi, J. Cao, M. S. Ryoo, and H. Kim, "Towards collaborative inferencing of deep neural networks on internet of things devices," *IEEE Internet of Things Journal*, 2020.
- [27] J. Mao, Z. Yang, W. Wen, C. Wu, L. Song, K. W. Nixon, X. Chen, H. Li, and Y. Chen, "Mednn: A distributed mobile system with enhanced partition and deployment for large-scale dnns," in *IEEE/ACM International Conference on Computer-Aided Design (ICCAD)*, 2017.
- [28] J. M. Tarnawski, A. Phanishayee, N. Devanur, D. Mahajan, and F. Nina Paravecino, "Efficient algorithms for device placement of dnn graph operators," *Advances in Neural Information Processing Systems*, 2020.